Analysis of experimental load dependence of two-dimensional atomic-scale friction

Satoru Fujisawa
Nanotechnology Division, Mechanical Engineering Laboratory, 1-2 Namiki, Tsukuba City 305-8564, Japan

Kousuke Yokoyama, Yasuhiro Sugawara, and Seizo Morita
Department of Electronic Engineering, Faculty of Engineering, Osaka University, 2-1 Yamada-Oka, Suita, Osaka 565-0871, Japan
(Received 6 October 1997; revised manuscript received 25 March 1998)

By using a two-dimensional frictional force microscope, we experimentally investigated and analyzed load dependence of atomic-scale friction between a single asperity tip and an atomically flat surface of graphite. While the tip shows the two-dimensional discrete jump between the sticking domains with the lattice periodicity in the higher load region, in the lower load region the tip shows rather smooth motion. The extent of the sticking domain decreases by increasing the load. Further, the appearance frequency of the zigzag motion of the discrete jump decreases by increasing the load. These results are explained by the load dependence of the effective adhesive region. [S0163-1829(98)02031-1]

I. INTRODUCTION

Friction always occurs at the sliding interface of two solids in contact. Since the friction is not only very important in technology but also a very interesting issue in science, its mechanism has been investigated by many researchers for a long time. To understand the basic mechanism of the friction, atomic-scale friction with a simple system, such as an atomically flat surface and a single asperity, has been explored in the past decade, both in numerous theoretical studies,[1–17] along with the recent development of the computed simulation, and in many experimental studies[18–27] by using a frictional force microscope.[18,20] On the other hand, as is pointed out by theoretical studies,[1,2] load is one of the most important parameters for the friction, which is deeply related to the mechanism of the friction. Thus, the experimental load dependence of atomic-scale friction should be investigated in more detail.

From our recent study on an atomic-scale friction between the single asperity and atomically flat surface by using the two-dimensional (2D) frictional force microscope (2D FFM), we found the two-dimensional discrete friction with the lattice periodicity. This phenomenon is explained by the two-dimensional stick-slip model.[28–33] The load dependence of this two-dimensional discrete friction has not, however, been adequately investigated. Therefore, in the present paper, we investigate and analyze the load dependence of the two-dimensional discrete friction in detail.

II. EXPERIMENTAL SETUP

By using a home-built atomic-force microscope (AFM) (Refs. 31 and 34), which works as a 2D FFM, we measured the displacements $(f_X/k_X, f_Y/k_Y)$ of a single asperity tip of AFM cantilever, by the raster scan. These displacements are caused by the two-dimensional frictional force vector (f_X, f_Y) between the tip and an atomically flat surface. k_X and k_Y are the spring constants of the AFM cantilever. Here we define X and Y directions as across and along the cantilever, respectively. The XY plane is parallel to the atomically flat surface. The Z direction is normal to the atomically flat surface. We used a weak feedback control in the Z direction in order to compensate for the slow Z direction drift. A cleaved (0001) surface of graphite (PGCCL) was used as an atomically flat sample surface, because it consists of only carbon atoms. The lattice structure exhibits threefold symmetry with a lattice constant of 0.246 nm. As the AFM cantilever, we used a rectangular microcantilever[35] that is made of Si_3N_4. The radius of curvature on the sharp tip apex is $\sim$20 nm. The tip height is 2.9 μm. The length, width and thickness of the cantilever are 100, 40, and 0.8 μm, respectively. The assumed elastic modulus and poisson ratio for the cantilever are 1.46×10^{11} N/m and 0.25, respectively. The calculated spring constants of the deflection and torsion of the cantilever are $k_Z=0.75$ and $k_X=550$ N/m, respectively.

To investigate the load dependence of frictional force, we increased the load step by step from 22 to $\sim$327 nN, and at each load we measured the frictional force image with the raster scan. The raster scan size is 1.3×1.3 nm. The raster scan rate was set at $\sim$21 nm/s for the fast line scan and $\sim$51 pm/s for the slow scan. The raster scan consists of 256 fast line scans. One of the lattice direction of the graphite surface was set to be parallel to the Y direction, i.e., fast line-scan direction. Soon after the cleavage of the graphite surface, measurements were performed in air at room temperature.

III. RESULTS AND DISCUSSION

A. Load dependence of force boundary in the frictional force image with the lattice periodicity

Figures 1(a)–1(d) show typical images of f_X/k_X (left) and f_Y/k_Y (right) at the loads of 22, 44, 91, and 327 nN, respectively. The lattice periodicity of the graphite surface appears in all of the images. Besides, by increasing the load, the pattern of the unit cell with the lattice periodicity changes drastically.

In order to characterize the drastic change of the unit-cell pattern in the images further, we focus on ''force boundary,'' where the brightness changes rather sharply. At the load of 22 nN, in the f_X/k_X image the vague force boundary indicates a dim triangular shape pattern toward the Y direction. In the f_Y/k_Y image the vague force boundary seems to show a dim honeycomb pattern. By increasing the load up to 44 nN, in both f_Y/k_Y and f_X/k_X images the force boundary

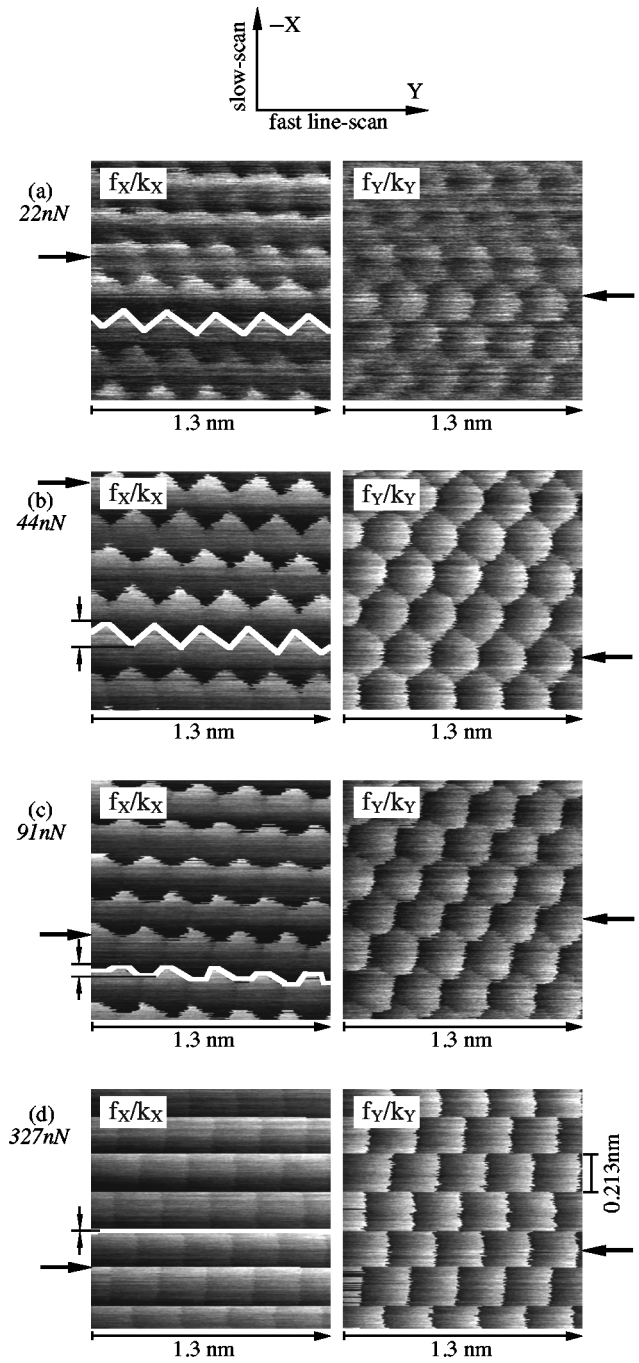

FIG. 1. Typical images of atomic scale friction at loads of (a) 22, (b) 44, (c) 91, and (d) 327 nN, by the raster scan. Left and right are the f_X/k_X and f_Y/k_Y images, respectively. The white line in the f_X/k_X image indicates the typical part of a shared force boundary with the f_Y/k_Y images.

becomes sharp and clear. In the f_X/k_X image, the force boundary shows a nearly triangular shape toward the Y direction. In the f_Y/k_Y image the force boundary shows a nearly honeycomb pattern. By increasing the load up to 91 nN, in the f_X/k_X image the force boundary shows a nearly trapezoid pattern in the Y direction. By comparing with the pattern at 44 nN, the top of the triangle appears to be removed or flattened. In the f_Y/k_Y image the force boundary shows a deformed hexagon. By increasing the load up to 327 nN, in the f_X/k_X image the force boundary shows a nearly straight line in the Y direction. By comparison with the pattern at 91 nN, the trapezoid pattern is completely flattened. In the f_Y/k_Y image the force boundary shows a nearly rectangular pattern.

By comparing the force boundary of the f_X/k_X image with that of f_Y/k_Y, we found that all of the force boundaries in the f_X/k_X image are shared with those in the f_Y/k_Y image. A typical part of this shared force boundary is roughly pointed out by a white line in the f_X/k_X image. The pattern of this shared force boundary is flattened from a triangular wave to a straight line by increasing the load. This flattering corresponds to decreasing of the slow-scan width at this shared force boundary, which is indicated by the small arrows on the left side of the f_X/k_X image. Here, the slow-scan width means the width or length for the slow-scan direction. On the other hand, the rest of the force boundary in the f_Y/k_Y image, which appears only in the f_Y/k_Y image, is a nearly straight line along the slow-scan direction. The straight line distributes with the lattice periodicity. By increasing the load, the length, i.e., the slow-scan width of the nearly straight lines, increases, resulting from the decrease of slow-scan width of the shared force boundary.

Consequently, by increasing the load from 22 to 44 nN, the force boundary becomes clear and sharp. Besides, by increasing the load from 44 to 327 nN, the pattern of the shared force boundary flattened by the change from a triangular shape to a straight line. Thus, a drastic change of the shared force boundary pattern by increasing the load from 22 to 327 nN is represented by increasing the clarity and sharpness of the force boundary and by decreasing the slow-scan width of the shared force boundary.

We mention that the observed load dependence of the lattice periodicity image agrees qualitatively with the computer simulated results, which assumes single-atom friction, performed by Sasaki and co-workers.[12,37,38] Thus, the experimental result seems to be explained qualitatively by the single-atom friction model. Also, the observed pattern change of the unit cell with the lattice periodicity seems to agree with the model of Kerssemakers and De Hosson,[13] if we assume that the magnitude of the frictional force increases with increasing load.

With the load from 22 to 327 nN, the contact area between the tip and graphite surface would be roughly made of more than several tens of atoms to several thousands of atoms, under the assumption that the strength of single covalent bond is of the order of 10^{-9} N.[39–41] Thus, to realize a two-dimensional stick-slip motion of the tip under the contact area of several thousands of atoms, we deduce that the graphite surface and its cleaved flake stuck to the tip generate two-dimensionally coherent or commensurate facial friction with the lattice periodicity of graphite, where the tip behaves like a single-atom tip.[18,28,32]

B. Load dependence of atomic-scale friction with the lattice periodicity

In order to study the mechanism of the observed load dependence of the force boundary in more details, we investigated all the fast line-scan data in all the experimental images. As a result, we found that the force boundary is formed by the slip signals, which is caused by the two-dimensional

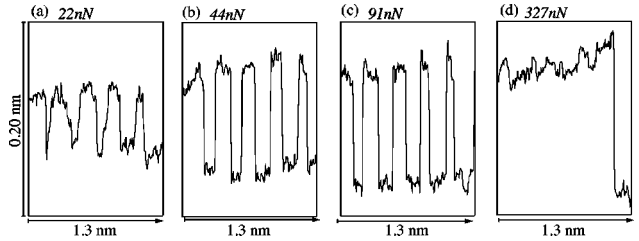

FIG. 2. Typical square-wave signals in the f_X/k_X images at loads of (a) 22, (b) 44, (c) 91, and (d) 327 nN. These data correspond to lines indicated by large arrows on the left sides of the f_X/k_X images in Fig. 1.

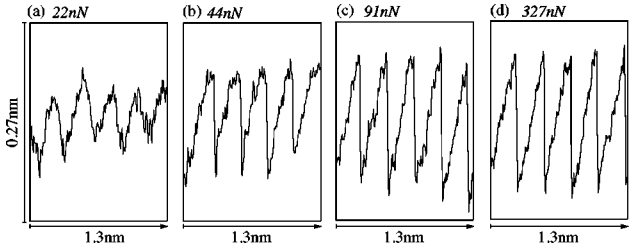

FIG. 3. Typical sawtooth signals in the f_Y/k_Y image at the loads of (a) 22, (b) 44, (c) 91, and (d) 327 nN. These data correspond to lines indicated by large arrows on the right sides of the f_Y/k_Y images in Fig. 1.

stick-slip motion of the tip.[28–33] Thus, it is suggested that the slip signal depends on the load.

Then, by investigating all the slip signals in all the images, we found that the increase of sharpness and clarity of the force boundary in the image corresponds to an increase of the sharpness and amplitude of the slip signal, which we discuss in the next subsection. Besides, we found that the decrease of the slow-scan width of the shared force boundary corresponds to a decrease of the appearance frequency with synchronized slip signal in the f_X/k_X and f_Y/k_Y images due to zigzag stick-slip motion of the tip, which we discuss in Sec. III B 2.

1. Load dependence of sticking domain with a definite extent

Figures 2(a)–2(d) show slip signals of typical fast line-scan data in the f_X/k_X image at loads of 22, 44, 91, and 327 nN, respectively. These data correspond to lines in the images in Fig. 1, which are indicated by large arrows on the left sides of the images. All of the data show the square-wave signals with the lattice periodicity. The amplitude of the slip signals increases by increasing the load. Furthermore at the load of 22 nN, the slope of the slip signals is not so sharp as those at 44, 91, and 327 nN, so that the wave form seems to be rather rounded.

Figures 3(a)–3(d) show the slip signals of typical fast line-scan data in the f_Y/k_Y image at the loads of 22, 44, 91, and 327 nN, respectively. These data correspond to lines in the images in Fig. 1, which is indicated by arrows on the right sides of the images. All of the data show sawtooth signals with the lattice periodicity. The amplitude of the slip signals increases by increasing the load. Furthermore, at the load of 22 nN, the slope of the slip signals is not as sharp as those at 44, 91, and 327 nN, so that the wave form seems to be rather rounded. On the other hand, at 22 and 44 nN the slope of the sticking signal is not as steep as those at 91 and 327 nN.

The amplitude of the slip signal corresponds to the slip distance of the tip between the stick points, according to the two-dimensional stick-slip model. So the measured slip distance should be smaller than the lattice constant of 0.246 nm, at least at a load smaller than 91 nN. This is not consistent with the assumption that the stick point is a point and slip distance is just the lattice constant in the simple two-dimensional stick-slip model. Therefore, we conjecture that the assumed stick point should not be a point but a region with a definite extent. We refer this region as a ''sticking domain.'' Further, from the increase of the amplitude of the slip signal by increasing the load, we expect that the extent of the sticking domain should decrease by increasing the load.

The sticking domain can be estimated by a spatial distribution of the tip position by the raster scan. The spatial distribution can be reconstructed from experimental data by converting the frictional force signals to the displacement of the tip, based on the method introduced by Kawakatsu and Saito[42,43] and Hölscher, Schwarz and Wiesendanger.[15,16,44,45] Figures 4(a)–4(d) show the spatial distributions of the tip position at the loads of 22, 44, 91, and 327 nN, respectively. These maps are obtained from corresponding images shown in Fig. 1. The tip position is indicated by the dot, where the existence frequency of the tip is indicated by the darkness. At a load of 22 nN, the distribution of the tip position is rather continuous and extends to the whole surface, although it seems to be a little concentrated with the lattice periodicity. This result suggests that the tip moves rather smoothly without stick-slip motion, although the tip motion has two-dimensionality with the lattice periodicity. By increasing the load up to 44 nN, the distribution of tip position becomes rather discrete with a clear lattice periodicity, which suggests a two-dimensionally discrete friction with the lattice periodicity. This discretely concentrated area of tip position corresponds to the sticking domain. This change of the sticking domain distribution from continuous to discontinuous by increasing the load seems to be similar to the change from *atomistic locking* to *dynamic locking*, which is theoretically predicted by Hirano and Shinjo.[2] By increasing the load by more than 44 nN, the extent of the sticking domain decreases as we expected.[12,37,38] On the other hand, even in the sticking domain the tip does not stick completely but moves gradually. Further, the rather smooth motion at the load of 22 nN could be interpreted such that the sticking domain extends to the whole area of the surface.

By comparing the typical fast line-scan data with the obtained tip position map, we conjecture that the round-shaped waves in both square-wave and sawtooth signals at 22 nN shown in Figs. 2(a) and 3(a) correspond to the smooth motion of the tip. Further, the gentle slope of the sticking signal in the sawtooth signal at 44 nN shown in Fig. 3(b) seems to correspond to the gradual motion of the tip in the sticking domain.

There is a possibility that a part of the observed motion of the tip is due to the lateral deformation of tip-sample contact or lateral bending of the tip.[46,47] The contribution of the lateral deformation or lateral bending is smaller than the actual tip motion. This is suggested from the result in Fig. 4 that the

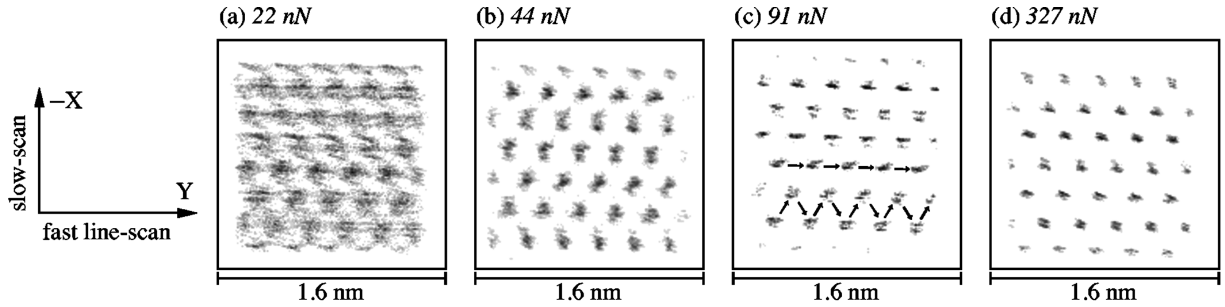

FIG. 4. Tip position maps at loads of (a) 22, (b) 44, (c) 91, and (d) 327 nN. These maps are converted from the f_X/k_X and f_Y/k_Y images shown in Fig. 1. The frame corresponds to 1.6×1.6 nm. A model of the straight and zigzag stick-slip motion of the tip is also superposed by the small arrows in (c).

observed tip motion becomes smaller, while the lateral deformation and bending should be larger, with the increase of the frictional force by increasing the load.

2. Transition from two-dimensional to one-dimensional frictions

By investigating all the slip signals in all the images, we found that the shared part of the force boundary with the f_Y/k_Y and f_X/k_X images is formed by synchronized slip signal appearing both in the f_Y/k_Y and f_X/k_X images. This synchronized slip signal is caused by the slip motion of the tip, which has both X and Y components, i.e., the zigzag stick-slip motion of the tip between the two rows of the sticking domain. A model of the zigzag stick-slip motion of the tip that is indicated by the small arrows is superposed in the spatial distribution of the sticking domain shown in Fig. 4(c). It should be noted that the rows of the sticking domain are along the Y direction. On the other hand, the rest of the force boundary in the f_Y/k_Y image is formed by the slip signal appearing only in the f_Y/k_Y image. This slip signal is caused by the slip motion that has only the Y component, i.e., the straight stick-slip motion of the tip along the Y direction through one row of the sticking domain. A model of the straight stick-slip motion of the tip is also superposed in Fig. 4(c) by the small arrows. Thus, the decrease of slow-scan width of the shared force boundary corresponds to the decrease of appearance frequency of the zigzag stick-slip motion of the tip, which results from the increase of the appearance frequency of the straight stick-slip motion of the tip.

As shown in Fig. 5, averaged appearance frequency of the zigzag stick-slip motion of the tip is estimated from the frictional force data shown in Fig. 1, as a function of the load. Three vertical thick bars and a dot (zero) shows experimental results at 44, 91, 122, and 327 nN, respectively. Here, $(\sqrt{3}/2)\times 0.246\ \text{nm} \fallingdotseq 0.213\ \text{nm}$ is the periodicity of the shared force boundary toward slow-scan direction, which is the orthography of the lattice periodicity for slow-scan direction. By increasing the load from 44 to 122 nN, the appearance frequency of the zigzag stick slip decreases almost linearly, which is indicated by dark area. Further, the dark area suggests the area of a possible two-dimensional state where the zigzag motion, i.e., the two-dimensional motion of the tip, may appear. On the other hand, the rest of the area suggests the area of possible one-dimensional state where the straight motion, i.e., one-dimensional motion of the tip may appear. Therefore, a remarkable transition from two to one-dimensional frictions on an atomic scale appears by increasing the load.[12,37,38]

In order to explain the mechanism of decrease of the appearance frequency of the zigzag stick-slip motion of the tip, we use a model of effective adhesive region (EAR) (Refs. 29, 30, 32) combined with the two-dimensional stick-slip model. First, we describe the definition of the EAR. Secondly, we clarify the condition for zigzag and straight stick-slip motions of the tip by using the model. Then, using the load dependence of the EAR, we explain the load dependence of appearance frequency of the straight and zigzag stick-slips of the tip. We mention that the frictional force data shown in Figs. 1–3 present the data just from the beginning of the fast line-scan including the onset region, i.e., the absolute magnitude of frictional force, which is essential

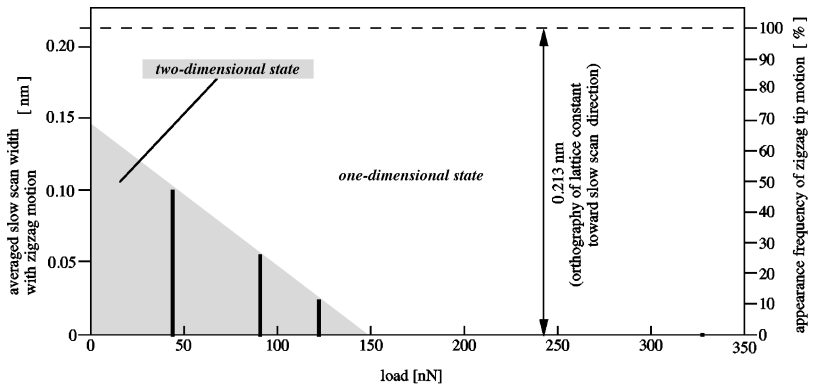

FIG. 5. Averaged width of slow scan with the zigzag stick-slip motion of the tip is plotted as a function of load, using vertical thick bars. Shaded area indicates estimated two-dimensional state where the zigzag motion, i.e., the two-dimensional motion of the tip, appears.

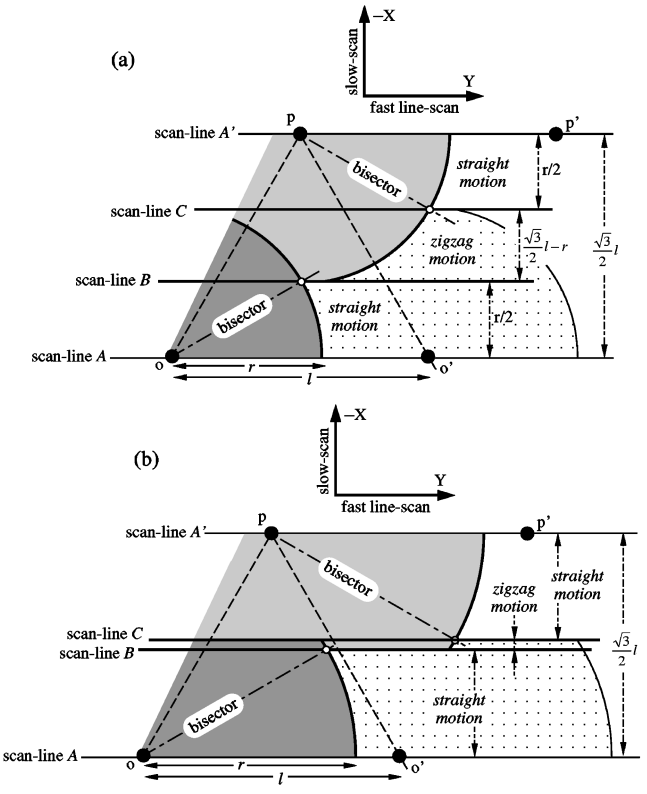

FIG. 6. EAR combined with the two-dimensional stick-slip model. The sticking domain and a part of its own effective adhesive region are represented by the concentric small filled circle and a part of a large dark circle, respectively. (a) shows the low load case in which the effective adhesive radius r is small, while (b) shows the high load case in which r is large. By comparing (a) and (b), the appearance frequency of the zigzag motion of the tip, i.e., the slow-scan width of the shared force boundary, decreases with increasing load.

for the EAR, as shown on Refs. 29, 30, and 32.

The EAR is defined by the area of the scan point when the tip sticks in its sticking domain. The scan point means the basal position of the tip under the assumption that the displacements of the cantilever spring for the X and Y directions are zero. In Fig. 6(a), for example, the sticking domain o and a part of its own EAR are represented by a concentric small filled circle and a part of a large dark circle, respectively. Here, to simplify the discussion, the shape of sticking domain and the EAR is assumed to be a circle, whose radius is r. The vector from the tip position in the sticking domain to the scan point represents the restored force of the cantilever spring. On the other hand, the vector from the scan-point to the tip position represents the sticking force due to the sticking domain, whose maximum is represented by the edge of EAR. So, when the scan point locates in the EAR, the two forces acting to the tip balances, which suggest that the tip is still sticking to the sticking domain. When the scan point, however, steps out of the edge of EAR by the fast line scan, the tip slips from its sticking domain to the next sticking domain, since the force of the cantilever spring overcomes the maximum sticking force. Therefore, we refer to this position of the scan point as the ''slip place.'' By the fast line scan, the trace of the scan point makes a line, namely, a ''scan line,'' which is represented by the solid line along the fast line scan. So, the slip place is the cross point of scan line and edge of EAR. By the slow scan, the slip place moves on the edge of the EAR, since the scan line moves in the X direction.

We make clear the condition for zigzag and straight stick-slip motions of the tip by using the EAR combined with the two-dimensional stick-slip model, as shown in Fig. 6. We focus on one period for the slow-scan direction from scan line A to scan line A', which has a distance of $(\sqrt{3}/2)l$. Here, scan line A is through the sticking domain o and o'. Scan line A' goes through sticking domain p and p'. The length l is a lattice periodicity of 0.246 nm. At first, the slip motion of the tip from sticking domain o, i.e., the EAR of sticking domain o, is discussed. The zigzag or straight slip motion of the tip corresponds to a jump of the tip to the sticking domain p or o', respectively. The condition that the tip jumps to the sticking domain p or o' is determined by which sticking domain, p or o', is closer to the slip place, because of the attractive force from the sticking domain to the tip during the slip motion.[30] So, depending on whether the scan line locates below scan line B or not, the tip takes a straight or zigzag motion, respectively. Here, scan line B goes through the cross point of the edge of EAR and the bisector of the o-p and o-o' lines. The cross point is represented by a small open circle. Then, the slip motion of the tip from sticking domain p is discussed. The zigzag or straight slip motion of the tip corresponds to jump of the tip to the sticking domain o' or p', respectively. The condition that the tip jumps to the sticking domain o' or p' is determined by which sticking domain, o' or p', is closer to the slip place. So, depending on whether the scan line is located above scan line C or not, the tip takes a straight or zigzag motion, respectively. The scan line C goes through the cross point of the edge of EAR and the bisector of the p-p' and p'-o' lines. Thus, in one period of $(\sqrt{3}/2)l$ for the slow-scan direction, the slow-scan width of the straight stick-slip motion is the summations of the distances from scan line A to scan line B and from scan line C to scan line A', which is equal to the effective adhesive radius (radius of EAR) r. So, the slow-scan width of the zigzag stick-slip motion is $(\sqrt{3}/2)l-r$.

Our previous study[30] made clear that by increasing the load, the r increases. As a result, the slow-scan width of straight stick-slip motion increases, while the slow-scan width of the zigzag stick-slip motion $(\sqrt{3}/2)l-r$ decreases, by increasing the load. Figure 6(a) shows the low load case that r is small, while Fig. 6(b) shows high load case that r is large. By comparing Figs. 6(a) and 6(b), the appearance frequency of the zigzag motion of the tip, i.e., the slow-scan width of the shared force boundary (distance between the scan-lines B and C) decreases with the increase of load, which well describes the change from Figs. 1(b)–1(d). Therefore, the load dependence of the EAR explains the increase of the appearance frequency of the straight stick-slip motion of the tip and resulting decrease of the appearance frequency of the zigzag stick-slip motion, by increasing the load.

C. Load dependence of effective adhesive radius

We qualitatively explain the load dependence of the effective adhesive radius using an interaction potential between a single-atom tip and monolayer surface correspond-

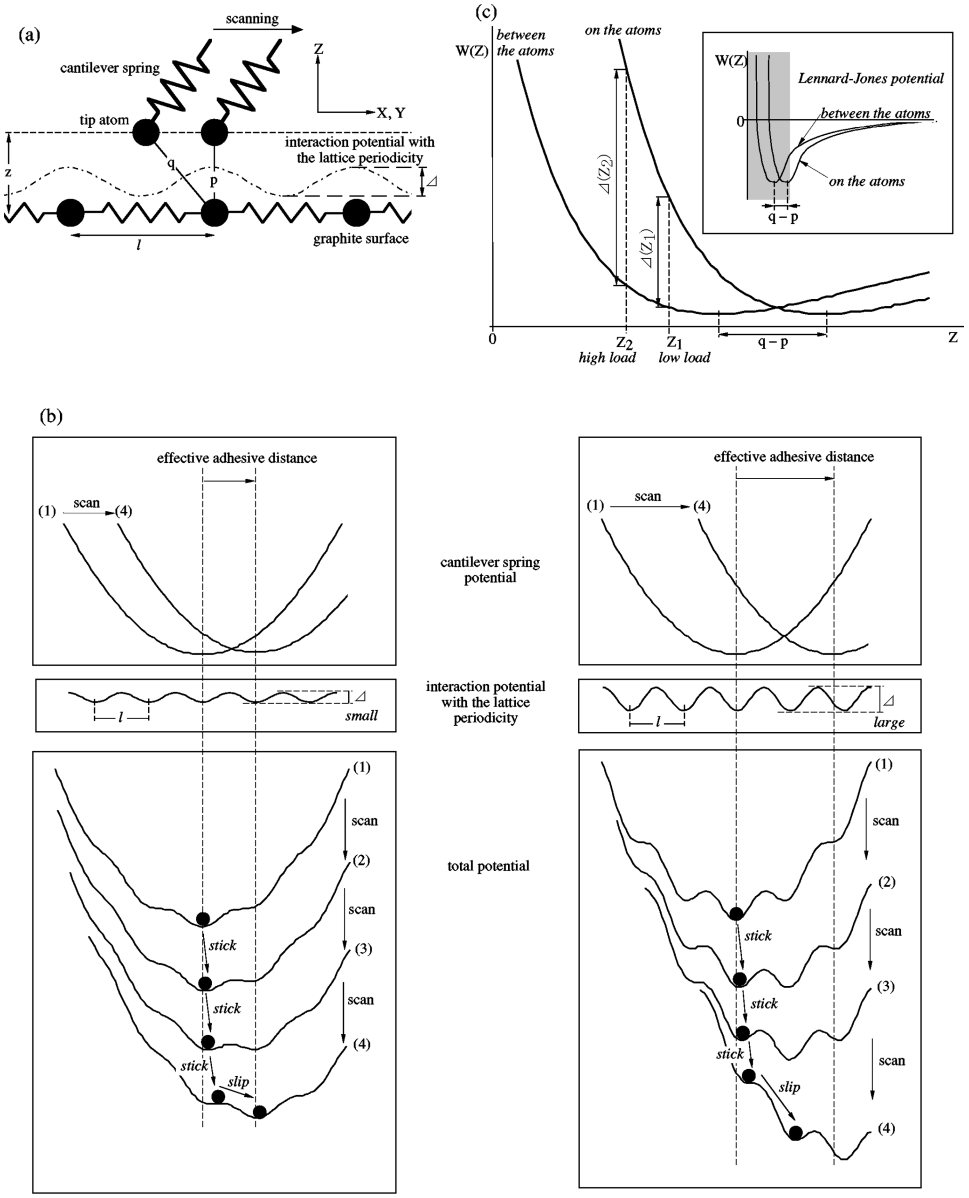

FIG. 7. (a) A simple one-dimensional model of a frictional force microscope with a single-atom tip and atomically flat surface. Closed circles represent the center position of the atoms. The sinelike wave shown by a dotted broken line represents the amplitude Δ of the interaction potential between the tip and surface. The dashed line shows the trajectory of the tip over the surface by the scanning. (b) shows the relation of the effective adhesive distance and amplitude of the interaction potential. The left and right figures show two cases in which the amplitude of the interaction potential Δ is small and large, respectively. The bottom part shows the summation of the cantilever spring potential (top part) and the interaction potential between the tip and the surface (middle part). (1)–(4) represent the evolution of the total potential by the scanning from (1) to (4). (c) shows two cases of Lennard-Jones potential $W(z)$ when the tip atom is above the places on and between the surface atom, as a function of the distance Z between the tip and surface in repulsive force region, which corresponds to enlarged figure of the shaded area of the inset graph.

ing to a simple one-dimensional model of the frictional force microscope, as shown in Fig. 7(a). Firstly, we explain that effective adhesive radius depends on the amplitude of the interaction potential by using energy minimization in a total potential model, in the next subsection. Then, the load dependence of the potential amplitude is explained by the Lennard-Jones potential between the tip and surface atoms, in Sec. III C 2.

Since the single-atom tip is used, the discussion regarding this model is limited to the behavior of single-atom friction and practical single-atom friction such as two-dimensionally coherent or commensurate friction between the layered material surface and its flake stuck to the tip, where we assume that the tip would move in similar way to the single-atom tip.[28,32]

1. Relation between the effective adhesive radius and the amplitude of the interaction potential

Figure 7(b) shows the total potential model of Fig. 7(a). In this one-dimensional model, the effective adhesive radius corresponds to the scanning distance required to cause the tip slip from the center of the sticking domain. We refer to this distance as the effective adhesive distance. The effective

adhesive distance is estimated by considering one stick-slip process of the tip with the evolution of the total potential by the scanning. The total potential is a summation of the cantilever spring potential and the interaction potential with the lattice periodicity. In the total potential model, the tip position corresponds to one of the local minima,[1,2,11–16,36–38,44,45] which is represented by the closed circle.

State (1) in Fig. 7(b) represents the state that the scan point locates at the center of a sticking domain. The scan point, which is represented by the vertical dashed line, indicates the basal position of the tip atom by the center of the parabola representing the cantilever spring potential. By the scanning, the scan point moves to the right, i.e., the relative position of the cantilever spring and the surface changes from (1) to (4) gradually. As the total potential evolves to (2) and (3), the local minimum where the tip stuck becomes shallower. At (4), the local minimum where the tip stuck from (1) to (3) disappears. It makes the tip jump or slip to the nearest local minimum. Thus, the effective adhesive distance corresponds to the scanning distance from (1) to (4), which is represented by the distance between the two vertical dashed lines. By comparing two cases with the small and large amplitudes of the interaction potential, as shown in the left and right hands in Fig. 7(b), the effective adhesive distance becomes larger as the amplitude increases.

It should be noted that by the evolution from (1) to (4) during the stick, the local minimum of the tip position moves gradually along the scanning direction. This small and slow motion of the tip corresponds to the gentle motion of the tip in the sticking domain, and gives a sticking domain a definite extent.

2. Load dependence of the amplitude of the interaction potential

The amplitude, i.e., the periodic change of the interaction potential with the lattice periodicity is qualitatively explained by the difference of the distance between the tip atom and surface atom. As shown in Fig. 7(a), the tip surface distance of $p\ (=z)$, where the tip atom is above the surface atom is shorter than q, where the tip atom is above the place between the surface atoms. So, based on the Lennard-Jones potential, the potential value between the tip and surface atoms changes depending on the tip position relative to the surface atoms, as shown in Fig. 7(c). This difference of Δ makes the potential amplitude with the lattice periodicity.[1,2,12,37] The Δ increases from $\Delta(Z_1)$ to $\Delta(Z_2)$, by decreasing the tip surface distance from Z_1 to Z_2 due to the increase of the load, as shown in Fig. 7(c). Thus, the potential amplitude increases by increasing the load.

We mention that in the two-dimensional stick-slip model a sticking force or attractive force works to the tip. The force between the tip and the surface is, however, repulsive, since the tip and the surface are in contact. This contradiction is explained by the fact that the weak place in the repulsive force distribution with the lattice periodicity appears to be a pseudoattractive place.

IV. CONCLUSION

We investigated the load dependence of an atomic-scale friction between a single asperity tip and atomically flat surface of graphite experimentally, by using a two-dimensional frictional force microscope. As a result, we found that the slip signal, which constructs the force boundary of the lattice periodicity image, changes drastically by increasing the load. From the load dependence of the slip signal, we found that the tip gradually moves while the tip sticks to the sticking domain. The extent of the sticking domain decreases by increasing the load. At low load region the sticking domain seems to cover the whole surface. Further, the appearance frequency of the zigzag stick-slip motion of the tip decreases by increasing the load, which is explained by the load dependence of the effective adhesive region. The origin of the load dependence of the effective adhesive region is attributed to the load dependence of the surface potential amplitude. These results are explained by the simple potential model between the tip and surface atoms.

ACKNOWLEDGMENTS

We thank Dr. T. Okada, S. Mishima, and S. Ito of Olympus Optical Co., Ltd. for the construction of the 2D-FFM unit. We also acknowledge A. Toda and K. Matuyama of Olympus Optical Co., Ltd. for supplying the Si_3N_4 microcantilevers. We especially thank E. Kishi for the adjustment and operation of the 2D-FFM system. We thank Dr. N. Sasaki of University of Tokyo for a useful discussion on the model of the atomic-scale friction. Part of this work was supported by a Grant-in-Aid for Scientific Research from the Ministry of Education, Science, Sports and Culture. A portion of this work was supported by the Research Development Corporation of Japan.

[1] G. M. McClelland, in *Adhesion and Friction*, edited by M. O. Grunze and H. J. Kreuser (Springer-Verlag, Berlin, 1990), p. 1.
[2] M. Hirano and K. Shinjo, Phys. Rev. B **41**, 11 837 (1990).
[3] U. Landman, W. D. Luedtke, and M. W. Ribarsky, J. Vac. Sci. Technol. B **9**, 414 (1991).
[4] J. A. Harrison, C. T. White, R. J. Colton, and D. W. Brenner, Phys. Rev. B **46**, 9700 (1992).
[5] J. A. Harrison, C. T. White, R. J. Colton, and D. W. Brenner, J. Phys. Chem. **97**, 6573 (1993).
[6] J. N. Glosli and G. M. McClelland, Phys. Rev. Lett. **70**, 1960 (1993).
[7] A. L. Shluger, A. L. Rohl, D. H. Gay, R. T. Williams, and R. M. Wilson, Phys. Rev. B **52**, 11 398 (1995).
[8] W. Zhong and D. Tomanek, Phys. Rev. Lett. **64**, 3054 (1990).
[9] D. Tomanek, in *Scanning Tunneling Microscopy III*, edited by R. Wiesendanger and H.-J. Güntherodt (Springer-Verlag, Berlin, 1993), p. 269.
[10] J. Colchero, O. Marti, and J. Mlynek, in *Forces in Scanning Probe Methods*, edited by H.-J. Güntherodt, D. Anselmetti, and E. Meyer (Kluwer Academic, Dordrecht, 1995), p. 345.
[11] Gyalog *et al.*, Europhys. Lett. **31**, 269 (1995).
[12] N. Sasaki, K. Kobayashi, and M. Thukada, Phys. Rev. B **54**, 2138 (1996).

[13] J. Kerssemakers and J. Th. M. De Hosson, J. Appl. Phys. **80**, 623 (1996).
[14] M. R. Sorensen, K. W. Jacobsen, and P. Stoltze, Phys. Rev. B **53**, 2101 (1996).
[15] H. Hölscher, U. D. Schwarz, and R. Wiesendanger, Europhys. Lett. **36**, 19 (1996).
[16] H. Hölscher, U. D. Schwarz, and R. Wiesendanger, Surf. Sci. **375**, 395 (1997).
[17] A. Buldum, S. Ciraci, and I. P. Batra, Phys. Rev. B **57**, 2468 (1998).
[18] C. M. Mate, G. M. McClelland, R. Erlandsson, and S. Chiang, Phys. Rev. Lett. **59**, 1942 (1987).
[19] R. Erlandsson, G. Hadziioannou, C. M. Mate, G. M. McClelland, and S. Chiang, J. Chem. Phys. **89**, 5190 (1988).
[20] G. Meyer and N. M. Amer, Appl. Phys. Lett. **57**, 2089 (1990).
[21] O. Marti, J. Colchero, and J. Mlynek, Nanotechnology **1**, 141 (1990).
[22] G. J. Germann, S. R. Cohen, G. Neubauer, G. M. McClelland, and H. Seki, J. Appl. Phys. **73**, 163 (1993).
[23] L. Howald, H. Haefke, R. Lüthi, E. Meyer, G. Gerth, H. Rudin, and H.-J. Güntherodt, Phys. Rev. B **49**, 5651 (1994).
[24] R. Lüthi, H. Haefke, E. Meyer, L. Howald, H.-P. Lang, G. Gerth, and H.-J. Güntherodt, Z. Phys. B **95**, 1 (1994).
[25] L. Howald, R. Lüthi, E. Meyer, and H.-J. Güntherodt, Phys. Rev. B **51**, 5484 (1995).
[26] R. M. Overney, H. Takano, M. Fujihira, W. Paulus, and H. Ringsdorf, Phys. Rev. Lett. **72**, 3546 (1994).
[27] R. W. Caripick and M. Salmeron, Chem. Rev. **97**, 1163 (1997).
[28] S. Fujisawa, Y. Sugawara, S. Ito, S. Mishima, T. Okada, and S. Morita, Nanotechnology **4**, 138 (1993).
[29] S. Fujisawa, E. Kishi, Y. Sugawara, and S. Morita, Phys. Rev. B **51**, 7849 (1995).
[30] S. Fujisawa, E. Kishi, Y. Sugawara, and S. Morita, Phys. Rev. B **52**, 5302 (1995).
[31] S. Fujisawa, E. Kishi, Y. Sugawara, and S. Morita, Tribol. Lett. **1**, 121 (1995).
[32] S. Morita, S. Fujisawa, and Y. Sugawara, Surf. Sci. Rep. **23**, 1 (1996).
[33] S. Fujisawa, Y. Sugawara, and S. Morita, Philos. Mag. A **74**, 1329 (1996).
[34] G. Binnig, C. F. Quate, and Ch. Gerber, Phys. Rev. Lett. **56**, 930 (1986).
[35] Olympus Optical Co., Ltd., 2951 Ishikawacho Hachioji, 192 Japan.
[36] N. Sasaki *et al.*, J. Vac. Sci. Technol. B **15**, 1479 (1997).
[37] N. Sasaki and M. Thukada, Sci. Rep. Res. Inst. Tohoku Univ. A **44**, 1 (1997).
[38] N. Sasaki *et al.*, Phys. Rev. B **57**, 3785 (1998).
[39] C. Kittel, *Introduction to Solid State Physics*, 6th ed. (Wiley, New York, 1986), Chap. 3, p. 71.
[40] M. Ohta, T. Konishi, Y. Sugawara, S. Morita, M. Suzuki, and Y. Enomoto, Jpn. J. Appl. Phys., Part 1 **32**, 2980 (1993).
[41] F. Ohnesorge and G. Binnig, Science **260**, 1451 (1993).
[42] H. Kawakatsu and T. Saito, J. Vac. Sci. Technol. B **14**, 872 (1996).
[43] H. Kawakatsu and T. Saito, in *Micro/Nanotribology and its Applications*, edited by B. Bhushan (Kluwer Academic, Dordrecht, 1996), p. 55.
[44] H. Hölscher, U. D. Schwarz, O. Zwörner, and R. Wiesendanger, Z. Phys. B **104**, 295 (1997).
[45] H. Hölscher, U. D. Schwarz, O. Zwörner, and R. Wiesendanger, Phys. Rev. B **57**, 2477 (1998).
[46] M. A. Lantz, S. J. O'Shea, A. C. F. Hoole, and M. E. Welland, Appl. Phys. Lett. **70**, 970 (1997).
[47] R. W. Carpick, D. F. Ogletree, and M. Salmeron, Appl. Phys. Lett. **70**, 1548 (1997).